Impact of bedding plane on tensile strength and fracture geometry derived from Brazilian tests on Montney equivalent rock discs

Seyed Hossein Tabatabaei Poudeh, Jeffrey A. Priest
Department of Civil Engineering – University of Calgary, Calgary, Alberta, Canada

ABSTRACT
Hydraulic fracturing (HF) or fracking is extensively used to increase the permeability of unconventional source rocks, such as the Montney formation which is prolific producer of oil and gas in Western Canada. Optimizing the economic recovery of hydrocarbons is dependent on understanding how these rocks fracture. However, failure mechanics of shale rocks are not well-understood due to the heterogeneous fabric (bedding) of the rock and their anisotropic stress-strain behaviour, which is rarely considered in geomechanical HF models. Recent studies have suggested that bedding plane weaknesses, and their orientation to the principal tensile stress, may influence how fractures form within the subsurface during HF stimulations. To investigate this behaviour, a series of Brazilian tests were conducted on Montney equivalent outcrop rock samples where the axial load was applied at different orientations to the bedding plane of the rock samples to investigate the influence of bedding plane orientation on fracture behaviour, including Brazilian tensile strength and fracture propagation. The results of this study can lead to better understanding of fracture behaviour of Montney shale and may help better predict HF fracture propagation and enhance hydrocarbon recovery.

RÉSUMÉ
La fracturation hydraulique (HF) ou fracking est largement utilisée pour augmenter la perméabilité des roches mères non conventionnelles, comme la formation Montney qui est un producteur prolifique de pétrole et de gaz dans l'Ouest du Canada. L'optimisation de la récupération économique des hydrocarbures dépend de la compréhension de la façon dont ces roches se fracturent. Cependant, la mécanique de la rupture des roches de schiste n'est pas bien comprise en raison de la structure hétérogène (stratification) de la roche et de leur comportement anisotrope en contrainte-déformation, qui est rarement pris en compte dans les modèles géomécaniques de la HF. Des études récentes ont suggéré que les faiblesses du plan de stratification, et leur orientation par rapport à la contrainte de traction principale, peuvent influencer la façon dont les fractures se forment dans la subsurface pendant les stimulations de la HF. Pour étudier ce comportement, une série d'essais brésiliens a été réalisée sur des échantillons de roche d'affleurement équivalents à ceux de Montney, où la charge axiale a été appliquée selon différentes orientations par rapport au plan de stratification des échantillons de roche, afin d'étudier l'influence de l'orientation du plan de stratification sur le comportement des fractures, notamment la résistance à la traction brésilienne et la propagation des fractures. Les résultats de cette étude peuvent conduire à une meilleure compréhension du comportement des fractures du schiste de Montney et peuvent aider à mieux prédire la propagation des fractures de la HF et améliorer la récupération des hydrocarbures.

1 INTRODUCTION

Unconventional oil and gas resources are playing an increasing role in meeting the energy needs of society. In Canada, it is estimated that up to 20×10^{12} m^3 of natural gas is stored in the Montney formation, a subsurface shale rock that spans the border between British Columbia and Alberta in Western Canada, and a prolific producer of oil and gas in Canada (NEB 2009). The Montney Formation is composed of multiple parasequence sets of fine to coarse grained siltstone, argillaceous siltstone and mudstone, and very fine-grained sandstone (Davies et al. 1997).

Due to the low permeability of shale rock, hydraulic fracturing (HF) is predominantly employed to enhance economic production of the oil and gas. HF models typically assume that fracture initiates when tensile stress exceeds the tensile strength of the isotropic media (Keneti and Wong 2010), and that the fractures develop perpendicular to the minimum in-situ stress direction within the formation. However, shale rocks are inherently anisotropic, where the rock exhibits different mechanical properties dependent on direction, which can be amplified by bedding planes. Results from Brazilian tests, where the rock is subject to tensile splitting, have indicated that the measured maximum failure stress depends on the angle between loading direction and bedding plane (Simpson et al. 2014; Yang et al. 2019), which also gives rise to different fracture patterns. Ignoring the rock anisotropic behaviour can therefore lead to significant errors in measured strength that can impact HF stimulation design. Therefore, a detailed fracture classification of rock formation being stimulated is necessary to better understand the failure modes and resultant stress magnitudes for the shale rock (Feng et al. 2020).

Experimental testing is the most reliable way to study the geomechanical properties and failure mechanism of the rock (Tavallali and Vervoort 2013; Vahdani et al. 2022). The tensile strength of a rock can be determined from

experimental methods either using direct and indirect tensile tests. As direct tensile testing is somewhat difficult and expensive, the Brazilian tensile test has been extensively used. The Brazilian test is an indirect test, in which a rock sample is subject to axial compressive stresses that induce tensile splitting of the rock. As the stress fields involved in rock formations, and in particular hydraulic fracturing, include combinations of compressive and tensile stress, the Brazilian tensile test is a desirable method due to its simplicity and lower costs. This test can also be used to investigate variations in tensile strength due to anisotropic behaviour (ASTM D3967 2016).

This study reports on a series of Brazilian tests that were conducted on samples of Montney equivalent outcrop rocks to investigate the anisotropic behaviour under different inclination of bedding plane angles (0 to 90˚). The results, including the Brazilian tensile strength (BTS), elastic properties, and fracture pattern of the rock, are presented, and discussed. In addition, a high-speed camera was utilized to investigate locations of fracture initiation and their propagation.

2 METHODOLOGY

In this section, the location of the rock outcrop and geological properties are described, along with sample preparation including sample dimensions. The Brazilian strength test is discussed including the derived formula to calculate the tensile strength from a Brazilian test.

2.1 Shale samples

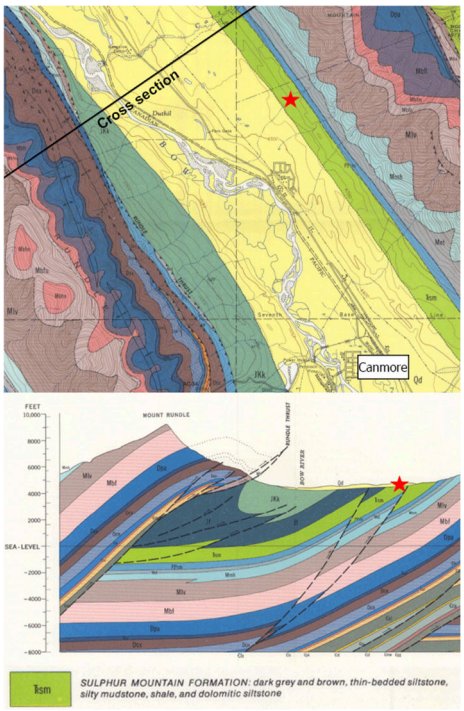

Figure 1. Geological map of Canmore (top) and layering cross section (bottom). Red star represents the study area (Price 1970).

The rock samples for the Brazilian tests were obtained from large rock boulders that were recovered from the Kamenka quarry located in Canmore, Alberta (Figure 1) where the Lower Triassic Sulphur Mountain Formation was exposed. This formation is considered to be age equivalent and geologically representative of the subsurface Montney Formation and therefore typically considered an analogue for characterizing the Montney (Zelazny et al., 2018).

Three core samples ~38 mm in diameter were drilled horizontal to bedding at different depths within a rock boulder obtained from the quarry (Figure 2), labelled A1, B1 and C1. These cores were subsequently cut perpendicular to the core length to obtain rocks discs for Brazilian testing. The cutting of each disc and subsequent polishing to ensure the ends of specimen were parallel (not exceeding 0.5˚ deviation across the sample ends) led to a nominal thickness of a rock disc of 13.9 mm with a standard deviation of 1.5 mm. All discs satisfied a thickness-to-diameter ratio (0.2 to 0.75) as defined in ASTM D3967. Thickness and diameter for each disc was determined from taking multiple measurements as shown in figure 3.

Figure 2. Rock block collected from quarry. Red circles represent the location of drilled cores for Brazilian tensile strength test.

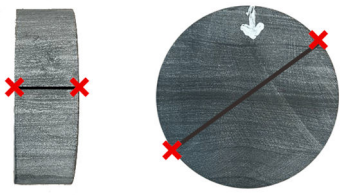

Figure 3. Illustration of a) thickness measurement b) diameter measurement (ASTM D3967 2016).

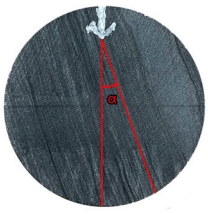

Figure 4. Test sample disk showing inclination angle of bedding planes with loading direction (α).

Samples were tested under axial loading with bedding planes orientated at different angles, α (α = 0˚, 15˚, 30˚, 45˚, 60˚, 75˚, and 90˚) to the loading direction (Figure 4) to investigate the effect of α on the Brazilian tensile strength. A strain gauge with a resistance of 120.0 ± 0.3 Ω and gage factor of 2.12 ± 1% (Tokyo Measuring Instruments I274-FLAB-6-11) were mounted centrally on each disk face, and either mounted vertically or horizontally (relative to the axial load) to measure both axial and radial strains to investigate the deformation behaviour of each disc.

2.2 Brazilian tensile strength test

Brazilian splitting tests were carried out using a servo-controlled MTS hydraulic load frame with a 100 kN inline load cell attached to the loading ram to measure axial load. Each disc was mounted between two stiff metal plates and subjected to an increasing axial load until failure. Cardboard cushions, with width of 5 mm and thickness of 0.38 mm, were used to reduce contact stresses and avoid stress concentration (ASTM D3967). The rock samples were subject to axial loading at a constant rate of displacement of 0.1 mm/min (measured by linear variable displacement transducer (LVDT) attached to the loading ram) to ensure tests were conducted under quasi static loading condition. Axial and radial strains measured by the strain gauges were simultaneously recorded, along with the applied axial load, at a rate of 10 hertz.

During the Brazilian test, the applied load increases up to the tensile failure of the disc, at which point a rapid drop in load is observed. From the maximum load that was recorded during the test the tensile strength of the rock can be calculated from:

$$\sigma_t = \frac{2P_{max}}{\pi D t} \qquad \text{(Eq. 1)}$$

Where σ_t is the Brazilian tensile strength (MPa), Pmax is the maximum applied load (N), D and t are the diameter and thickness of the sample (mm), respectively (ASTM D3967 2016).

Equation 1 is based on linear elastic theory for homogenous and isotropic rock that is diametrically loaded resulting in vertical splitting of the discs. Although shale rocks are heterogeneous, transversely isotropic in nature and do not typically exhibit singular vertical splitting (Yang et al. 2019; Feng et al. 2020). However, this equation is used simply for the purpose of comparison of tensile strength as a function of bedding plane inclination.

3 RESULTS AND ANALYSIS

In this section the results from Brazilian tensile tests on 21 samples (seven bedding plane orientations from 3 different depths) are discussed. Tensile strength, vertical and horizontal strains and elastic properties determined from each test are considered. In addition, fracture formation and fracture patterns are classified.

Figure 5 shows the typical load-deformation history for a single test, where axial load is given by the load cell and displacements given by the LVDT attached to the loading ram. Before the start of the test an initial nominal seating load of 0.35 kN is applied. As the test progresses axial load increases with displacement of the loading ram, until tensile splitting (failure) of the sample occurs corresponding to a rapid drop in axial load. The resolution of the LVDT (50 mm full scale) leads to the jagged response in the load-deformation curve. Figure 6 compares the strains calculated from the LVDT and those measured by the strain gauges. Firstly, it can be seen that the strain gauges give greater resolution than the LVDT, along with measuring only the strains in the rock sample, rather than the cardboard strips, which was used to avoid stress concentration and achieve the realistic tensile failure. The splitting of the disc typically breaks the strain gauges, which leads to an abrupt change in strain at around 260 seconds. For analysis, the peak axial load and corresponding strain at the point the disc breaks are used.

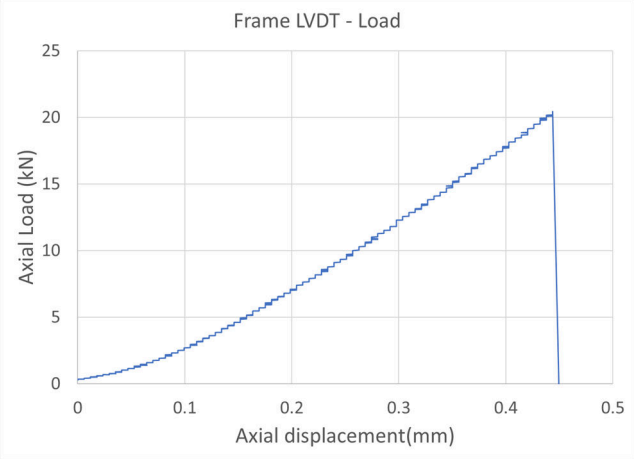

Figure 5. Plot of frame LVDT against load based on raw data.

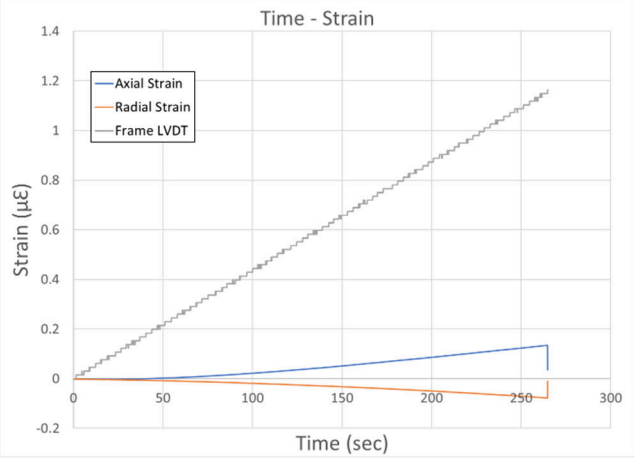

Figure 6. Comparison of strain gauges strains and LVDT.

3.1 Brazilian tensile strength

The variation in Brazilian tensile strength (calculated using Eq. 1) with inclination angle is shown in Figure 7 for all samples tested, with Table 1 highlighting the mean, maximum and minimum tensile strength recorded for each core. It can be seen that each group of samples exhibit a degree of scatter in tensile strength. Lines of best fit through each data set show a weak association with inclination angle as highlighted by the R-squared value derived from the best fit lines. Core C1 exhibited the largest variability in strength with a mean of 23.1 MPa, and a maximum and minimum strength of 27.9 MPa and 17.7 MPa, respectively. However, the line of best fit had the highest R-squared value.

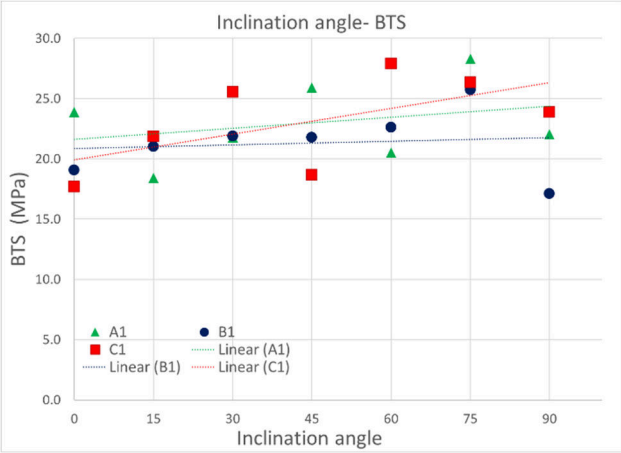

Figure 7. Variation in Brazilian tensile strength with inclination angle for different bedding planes.

Table 1. Summary of BTS results showing mean, standard deviation, R-squared, maximum, and minimum values.

Bedding plane	Mean (MPa)	SD[1] (MPa)	R^2	Max BTS (MPa)	Min BTS (MPa)
A1	23	3.3	0.09	28.3	18.4
B1	21.3	2.7	0.01	25.7	17.1
C1	23.1	3.9	0.35	27.9	17.7

[1]Standard deviation

Considering B1, which has a mean of 21.3 MPa, and a maximum and minimum strength of 25.7 MPa and 17.1 MPa, there appears to be an increase in strength with inclination angle until α=90° where there is a sudden reduction of 8.6 MPa in strength. Close inspection of the samples after testing typically showed vertical fractures (Figure 8c). However, for sample B1 tested at an inclination angle of α=90°, a premature fracture occurred towards the edge of the sample before the sample failed (Figure 8a). This might suggest that this sample was damaged. Ignoring this sample and fitting a line of best fit through the remaining data shows a stronger relationship between tensile strength and bedding plane orientation, with an R-squared value of 0.86.

Yang et al. (2018) showed that inclination angle influenced the strength measured for Changsha shale, with BTS increasing from 4.3 MPa at α=0° to a maximum BTS of 11.98 MPa at α=75° which shows an increase of 178% from minimum to maximum value. However, the results from the study presented in this paper do not show any systematic change of BTS with inclination angle. In addition, the measured variation in strength was much reduced, varying by 54% for A1, 49% for B1 and 60% for C1. Thus, the tested samples appear to not exhibit strong anisotropy which might be due to the rock fabric and depositional setting of bedding planes.

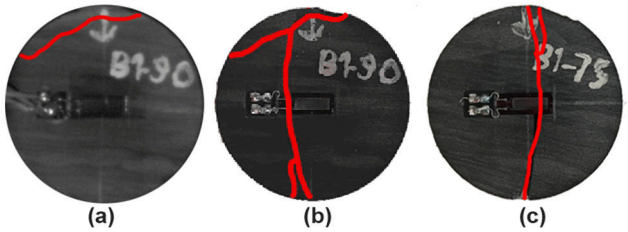

Figure 8. (a) A premature fracture in B1-90 before complete failure of sample. (b) Complete fracture pattern in B1-90 at sample failure. (c) A typical fracture pattern at sample failure.

3.2 Axial and lateral strains

Figures 9, 10 and 11 show measured axial and radial strains developed on the disc face with tensile strength for samples from A1, B1 and C1, respectively. Generally, axial strains exhibit higher variability compared to radial strains, with core samples of B1 having the largest variability both in axial and radial strains compared A1 and C1.

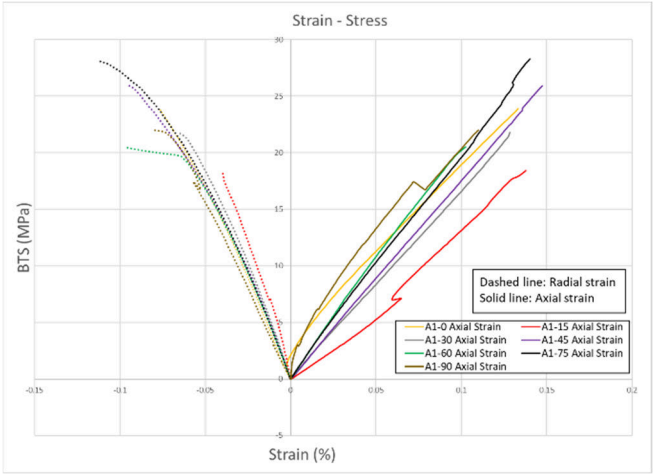

Figure 9. Axial and radial strain with tensile strength for A1 samples from Brazilian tests.

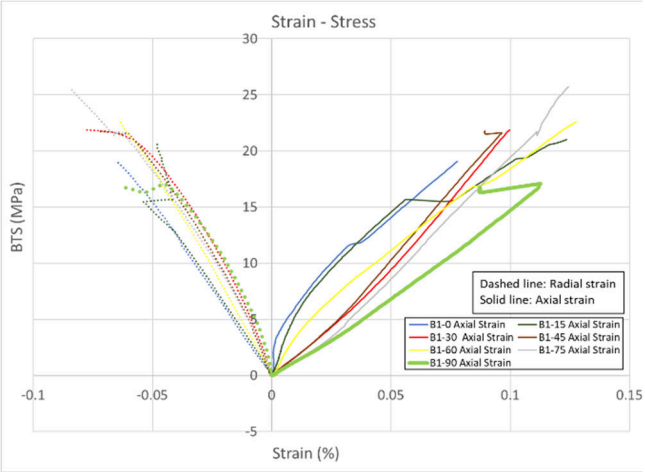

Figure 10. Plot of axial and radial strain against BTS for B1.

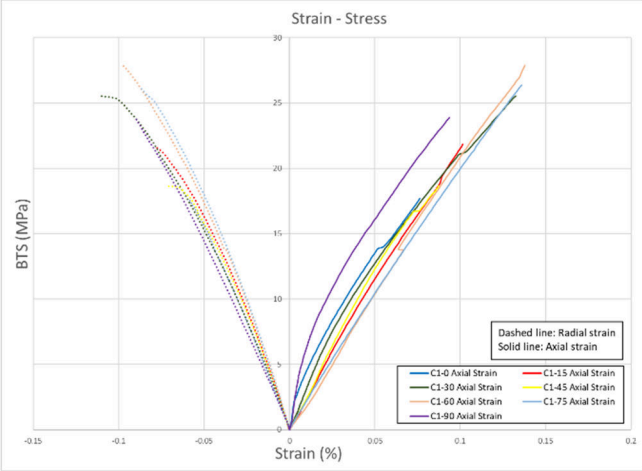

Figure 11. Plot of axial and radial strain against BTS for C1.

In comparing axial and radial strain response it appears that samples with higher axial strains for a given load (least stiff) developed the lowest radial strains, while samples with the least axial strain for a given load (stiffest) showed the highest radial strains. This relationship can be seen when comparing core sample A1-15 with A1-90 (Figure 9), core sample B1-90 with B1-0 (Figure 10) and C1-75 with C1-90 (Figure 11). However, no correlation appeared to exist between maximum axial or radial strain with maximum tensile.

Although the strain data is truncated at the point of failure of disc, tracking the axial and radial strains can be used as an indicator of strain localization where small fractures inside the disk might occur and ultimately lead to primary fracture. For example, there is a sudden change in strain and a marginal reduction in strength for B1-90 (Figure 10-bold green line) which occurs before complete failure.

3.3 Elastic properties of rock discs

The elastic properties of rocks, such as Young's modulus and Poisson's ratio, are important parameters used for characterizing the geomechanical behaviour of rocks, and used for understanding formation behavior HF stimulations. For example, a rock with a high Young's modulus, typically exhibits a high net breakdown pressure and more extensive fracture networks during HF stimulation compared to rocks with lower Young's modulus. Poisson's ratio is used also in determining the brittleness and subsurface behaviour of rock (McKean and Priest 2019; Smith et al. 2001). The degree of rock anisotropy can be investigated from the stress-strain behaviour of rocks and the derived rocks elastic properties.

Different methods can be used for determining the elastic modulus of a rock from the gradient of the stress-strain curve. The different methods, such as tangent modulus, secant modulus and linear modulus, depend on the respective end points of the stress-strain curve that the gradient is measured over. As the stress strain curves are typically non-linear, the different estimates of the elastic modulus can vary considerably. As such, values are typically determined from the gradient of the curve at a defined point, such as 50% of the ultimate tensile strength. In this paper, the linear modulus is determined from fitting a straight line to the linear region of the curve at 50% ultimate stress.

Figure 12 and 13 presents the elastic modulus obtained from both the compressive and radial stress-strain response as a function of inclination angle of bedding plane. Similar to that obtained from tensile strength, the fitting of trendlines shows that there is a fairly weak association between elastic modulus and inclination angle. For the elastic modulus derived from axial load, A1 samples show an increase in elastic modulus with inclination angle, while both B1 and C1 suggest the reverse, that is a reduction in stiffness. In contrast, for the modulus from tensile stress and radial strain, A1 and C1 highlight a reducing stiffness while B1 shows an increasing stiffness.

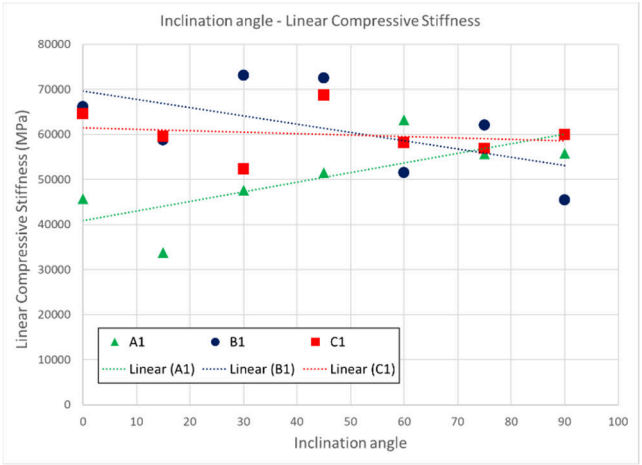

Figure 12. Plot of linear compressive modulus against inclination angle in different bedding planes.

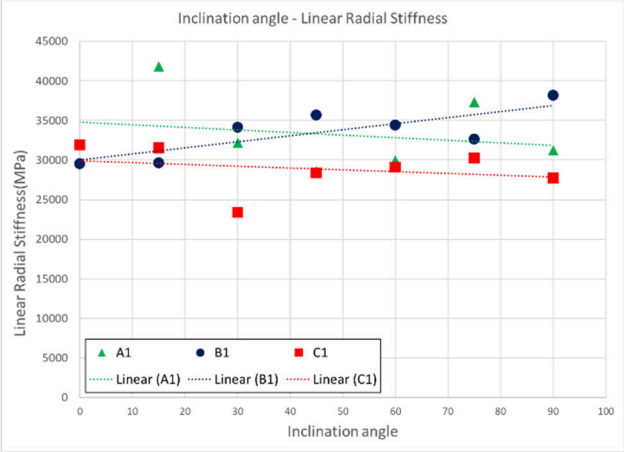

Figure 13. Plot of linear radial modulus against inclination angle in different bedding planes.

From the ratio of radial strains with axial strains the Poisson's ratio for the rock samples can be determined. Figure 14 shows significant variability in Poisson's ratio for the three core samples as a function of inclination angle. For most isotropic rocks a Poisson's ratio of 0.2-0.3 would typically be expected, however from the tests conducted the calculated values range from 0.2 – 0.9. The data at C1-90 was removed since it was out of range of Poisson's ratio. For A1 samples, Poisson's ratio increases to 0.25 at α=15° and 0.66 at α=90°. However, B1 samples show the reverse behavior with a Poisson's ratio of 0.35 at α=90° and 0.85 at α=0°. C1 does not show any appreciable trend with Poisson's ratio of 0.58 and 0.87 for α=75° and α=90°, respectively.

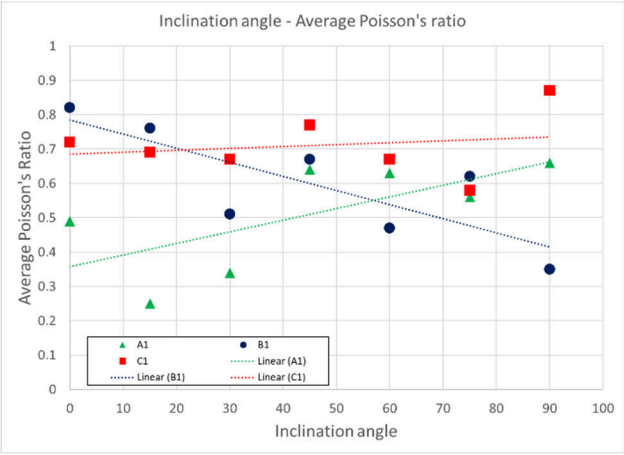

Figure 14. Plot of average Poisson's ratio against inclination angle in different bedding planes.

3.4 Fracture analysis

3.4.1 Fracture tracing

From the results presented above it can be seen that although there is significant variation in measured tensile strength and elastic properties, there does not appear to be any significant correlation between these measurements and inclination angle. However, the tensile strength, and the strain that is measured, appear to be related to the fracturing of the rock discs. To track fracture behaviour during loading a VEO-E 340L high speed camera, which has a maximum frame rate of 19000 fps (frames per second), was used to capture the onset and growth of fractures in a disc. The camera is manually started to record prior to the occurrence of peak strength and ~ 6 seconds of loading is recorded. Figure 15 shows a sequence of frames that capture the initiation of a tensile fracture and its propagation during the testing of sample B1-60. The first image (given a time stamp 1/19000 sec) is the first frame immediately before a fracture is observed. Subsequent images capture the rapid evolution of the fracture through the sample. In most tests the onset of fracturing initiates at the center of the specimen (Figure 15-b) and extends outwards along the loading direction (vertically). Secondary fractures subsequently form and connect with the primary fracture to form a complex fracture network. The time from initiation of a fracture to the eventual sample failure took less than 210 microseconds (μs) to occur, that gave a fracture propagation velocity estimated to be 182 m/sec (assuming half disc diameter).

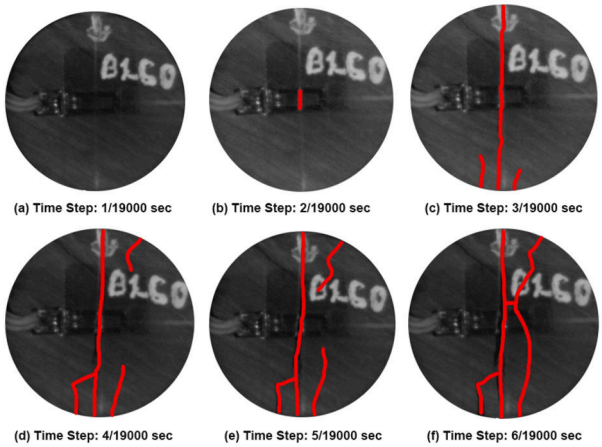

Figure 15. Fracture initiation and propagation starting from one frame before fracture initiation at the center of specimen (a) until multiple fracture formation (f).

3.4.2 Fracture Propagation

The following classification scheme developed by Tavallali and Vervoort (2013) was used to analyse the fracture:

1. Central fracture (CF): A fracture develops roughly parallel to the loading direction and is bounded within the central portion of the sample defined as 10% of the diameter on either side of the centerline.
2. Layer activation (LA): Fractures propagate along the bedding plane.
3. Non-central fracture or arc fracture (AF): Fractures extend outside of central portion of the disc, and not associated with bedding plane activation.

For an inclination angle, α=0 a fracture that occurs parallel to the bedding planes is classified as layer activation and not central fracture.

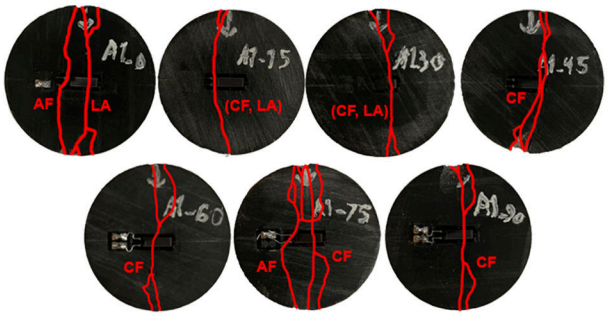

Figure 16. Fracture paths observed for A1 samples (represented by red lines). predominant fracture mode is given with the secondary fracture mode given in parentheses.

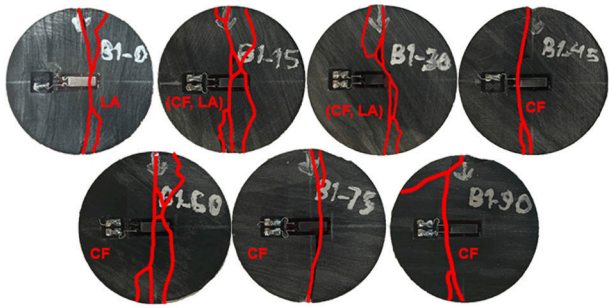

Figure 17. Fracture paths observed for B1 samples (represented by red lines). predominant fracture mode is given with the secondary fracture mode given in parentheses.

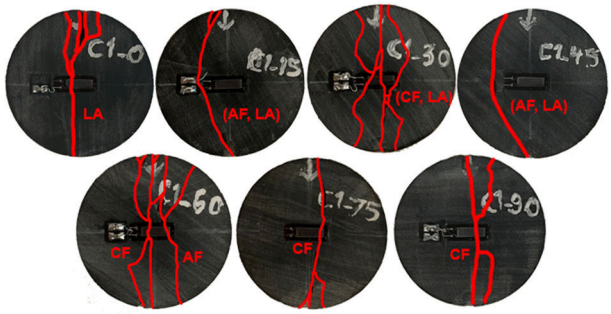

Figure 18. Fracture paths observed for C1 samples (represented by red lines). predominant fracture mode is given with the secondary fracture mode given in parentheses.

As shown in figure 16 - 18, all samples exhibited a range of fracture patterns with no systematic fracture pattern associated with inclination angle. In addition, no systematic fracture pattern was observed between samples (different bedding planes) except the inclination angle of 30 (CF and LA type) and 90 (CF type).

The propagated fractures were typically 'through sample' so that the fracture patterns observed on the front and rear faces of the disc were similar although not exact, which suggests minor differences in rock fabric in the plane over the disc depth. However, a number of samples exhibited significantly different fracture pattern between the front and back suggesting a heterogenic fabric, for example, Sample B1-90 where on front side an AF fracture type was observed and CF type on the back side (Figure 19).

Figure 19. Illustration of fracture pattern in front side and back side of B1-90 indicating a three-dimensional fabric.

4 DISCUSSION

Previous research on the behaviour of layered rock such as shale and sandstone indicate increasing tensile strength as a function of inclination angle (Tavallali and Vervoort 2013; Yang et al. 2019; Feng et al. 2020). However, the results from samples tested in this study do not show any strong trends with inclination angle and exhibit high variability across the different inclination angles and different bedding planes (Figure 7). Although bedding planes can be seen in the samples tested, fractures typically did not occur along the bedding plane at different inclination angle. This suggests that for samples tested the bedding planes were not a determining factor in observed fracture patterns or strength.

Inherent anisotropy can arise due to microscopic and petrographic characteristics of rock, such as grain size, mineralogy, degree and type of cementation and degree of compaction. Therefore, these aspects may need to be investigated to better understand the anisotropy behaviour of samples (Yin and Yang 2018).

According to Tavallali and Vervoort (2010), higher strength is associated with increasing total fracture length. Table 2 presents the strength measured on samples from core A1 along with the observed fractures. It can be seen that the fracture complexity increases with BTS. Samples with low strength typically gave rise to one central fracture or exhibited layer activation. However, sample with highest strength comprises multiple fractures. The results suggest that for the samples tested higher strength is correlated with fracture complexity, which might be due to the rock fabric rather than inclination angle.

Table 2. BTS values and corresponding fracture pattern for core A1.

.

BTS (MPa)	18.4	20.5	21.8	22	23.9	25.9	28.3
Fracture complexity				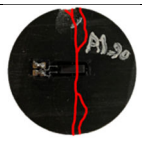	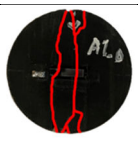		

5 CONCLUSIONS

Brazilian tensile tests were conducted on numerous Montney equivalent outcrop samples that had different bedding planes to investigate the possible influence of bedding plane orientation on the geomechanical properties and fracture patterns of the rock discs. Based on the results presented the following conclusions are drawn:

1- Variability in tensile strength is evident that is not associated with inclination angle and may result from inherent anisotropy of the rock.
2- Elastic properties, such as elastic stiffness and Poisson's ratio, were evaluated as a function of different inclination angle. Similar to strength, significant variability was observed in elastic properties that was not associated with bedding plane orientation.
3- Fracture propagated rapidly once initiated occurring in less than 210 µs as recorded by high-speed camera. The fracture velocity was estimated at around 182m/sec.
4- No systematic fracture patterns were observed with bedding plane inclination angle, with samples exhibiting a mix of fracture types.
5- Increasing fracture complexity was observed with increasing strength rather than inclination angle.

This study shows that the geomechanical properties and fracture pattern of shale rocks appear to exhibit strong anisotropy. This may need to be considered in HF design to effectively stimulate the shale reservoirs.

6 REFERENCES

ASTM. 2016. D3967-16: standard test method for splitting tensile strength of intact rock core specimens. ASTM International, West Conshohocken, PA. doi:10.1520/D3967-16.

ASTM, 2014, D7012-14: standard test methods for compressive strength and elastic moduli of intact rock core specimens under varying states of stress and temperatures: West Conshohocken, PA. doi:10.1520/D7012-14.

Davies, G.R., Moslow, T.F., and Sherwin, M.D. 1997. The Lower Triassic Montney Formation, west-central Alberta. Bulletin of Canadian Petroleum Geology, 45(4): 474–505. doi:10.35767/gscpgbull.45.4.474.

Feng, G., Kang, Y., Wang, X., Hu, Y., and Li, X. 2020. Investigation on the Failure Characteristics and Fracture Classification of Shale Under Brazilian Test Conditions. Rock Mechanics and Rock Engineering, 53(7): 3325–3340. doi:10.1007/s00603-020-02110-6.

Keneti, S.A., and Wong, R.C. 2010. Investigation of Anisotropic Behaviour of Montney Shale Under Indirect Tensile Strength Test. p. SPE-138104-MS.

McKean, S.H., and Priest, J.A. 2019. Multiple failure state triaxial testing of the Montney Formation. Journal of Petroleum Science and Engineering, 173: 122–135. doi:10.1016/j.petrol.2018.09.004.

NEB. 2020. A Primer for Understanding Canadian Shale Gas. National Energy Board, Calgary, Alberta, Canada. November.

Price R.A., 1970b, Geology, Canmore (west half), west of Fifth Meridian, Alberta: Geological Survey of Canada "A" Series Map 1266A, scale 1:50,000.

Simpson, N.D.J., Stroisz, A., Bauer, A., Vervoort, A., and Holt, R.M. 2014. Failure Mechanics of Anisotropic Shale During Brazilian Tests. p. ARMA-2014-7399.

Smith, M.B., Bale, A.B., Britt, L.K., Klein, H.H., Siebrits, E., and Dang, X. 2001. Layered Modulus Effects on Fracture Propagation, Proppant Placement, and Fracture Modeling. p. SPE-71654-MS.

Tavallali, A., and Vervoort, A. 2010. Effect of layer orientation on the failure of layered sandstone under Brazilian test conditions. International Journal of Rock Mechanics and Mining Sciences - INT J ROCK MECH MINING SCI, 47: 313–322. doi:10.1016/j.ijrmms.2010.01.001.

Tavallali, A., and Vervoort, A. 2013. Behaviour of layered sandstone under Brazilian test conditions: Layer orientation and shape effects. Journal of Rock Mechanics and Geotechnical Engineering, 5(5): 366–377. doi:10.1016/j.jrmge.2013.01.004.

Vahdani, M., Hajitaheriha, M.M., Hasani Motlagh, A., and Sadeghi, H. 2022. A Modified Two-Surface Plasticity Model for Saturated and Unsaturated Soils. Indian Geotechnical Journal,: 1–12. Springer.

Yang, S.-Q., Yin, P.-F., and Huang, Y.-H. 2019. Experiment and Discrete Element Modelling on Strength, Deformation and Failure Behaviour of Shale Under Brazilian Compression. Rock Mechanics and Rock Engineering, 52(11): 4339–4359. doi:10.1007/s00603-019-01847-z.

Yin, P.-F., and Yang, S.-Q. 2018. Experimental investigation of the strength and failure behavior of layered sandstone under uniaxial compression and Brazilian testing. Acta Geophysica, 66(4): 585–605. doi:10.1007/s11600-018-0152-z.

Zelazny, I.V., Gegolick, A., Zonneveld, J.-P., Playter, T., and Moslow, T.F. 2018. Sedimentology, stratigraphy and geochemistry of Sulphur Mountain (Montney equivalent) Formation outcrop in south central Rocky Mountains, Alberta, Canada. Bulletin of Canadian Petroleum Geology, 66(1): 288–317.